Int. J. Solids Structures Vol. 28, No. 8, pp. 975–1001, 1991
Printed in Great Britain.

0020–7683/91 $3.00 + .00

EFFECT OF INCLUSION SHAPE ON STIFFNESS OF ISOTROPIC AND TRANSVERSELY ISOTROPIC TWO-PHASE COMPOSITES

B. J. LEE and M. E. MEAR
Department of Aerospace Engineering and Engineering Mechanics,
The University of Texas at Austin, Austin, TX 78712, U.S.A.

(*Received* 18 *June* 1990; *in revised form* 2 *February* 1991)

Abstract—Constitutive relations are developed for linear and non-linear incompressible, two-phase composites. The second phase is assumed to be comprised of spheroidal inclusions, and both isotropic composites (containing randomly oriented inclusions) and transversely isotropic composites (containing aligned inclusions) are examined. Constitutive relations are established first for linearly elastic constituents and dilute concentrations of inclusions. Corresponding (approximate) constitutive relations applicable for non-dilute concentrations of inclusions are then obtained using a differential self-consistent scheme. Next, constitutive relations for non-linear matrix materials are developed using a procedure recently introduced by Ponte Castaneda [*J. Mech. Phys. Solids* (1991)]. The procedure uses a variational framework to exploit the constitutive relations developed for linear matrix behavior in order to obtain approximate results for non-linear matrix behavior. The results obtained are rigorous bounds on the behavior of the composites when the concentration of inclusions is sufficiently small, and are estimates for the behavior at larger concentrations of inclusions. The constitutive relations established for linear and non-linear composites are used to examine the effect of inclusion shape on the stiffness of composites, and a wide range of inclusion shapes ranging from thin disk-shaped inclusions to slender needle-like inclusions is considered.

1. INTRODUCTION

The mechanical properties of a material may be enhanced through the introduction of a second phase material. Among the properties of interest is the stiffness of the composite. It should be expected that the introduction of a (well bonded) second phase which has a stiffness greater than the matrix material will give rise to a composite material which has a net stiffness larger than that for the pure matrix material. The amount of stiffening which is achieved in this way depends, naturally, on the relative stiffness of the second phase and its volume fraction in the composite, but it also depends on the shape of the second phase inclusions.

For linearly elastic constituents, there have been many studies performed to determine bounds or estimates for the moduli of two-phase composites (see, e.g., the review articles of Hashin, 1983; Willis, 1983), but there have been relatively few efforts aimed at exploring the effect of particle shape on the stiffness of the composite. The first appears to be the study by Wu (1966), who used the self-consistent scheme developed by Budiansky (1965) and Hill (1965) to obtain estimates for the moduli of composites in which the inclusions are randomly oriented. He explicitly examined the case of spherical inclusions and the limiting cases of flat platelets and infinitely long circular cylindrical inclusions, concluding that the platelets give rise to the largest stiffening effect. Tandon and Weng (1984) examined the effect of inclusion aspect ratio on the moduli when the inclusions are aligned, and later Tandon and Weng (1986) extended the work to the case of randomly oriented inclusions. In their studies, the Mori–Tanaka (1973) procedure was used to obtain estimates for the moduli of specific two-phase systems of interest.

For non-linear matrix materials, procedures for obtaining bounds on the constitutive behavior have recently been developed (e.g. Ponte Castaneda and Willis, 1988; Ponte Castaneda, 1991) and these have been used to examine composites comprised of non-linear matrix materials containing spherical inclusions. The effect of inclusion shape on the stiffness of non-linear composites has been examined by Lee and Mear (1991) for the case in which the inclusions are aligned. They obtained accurate constitutive relations for power-law matrix materials containing rigid spheroidal inclusions, but their analysis was restricted to

axisymmetric loading of the composite (with the symmetry axis of the loading coinciding with the direction of alignment of the inclusions). Approximate constitutive relations for aligned and randomly oriented inclusions in a plastically deforming matrix have also been developed recently by Zhao and Weng (1990) and Qiu and Weng (1990), respectively.

The purpose of the present investigation is to give a more comprehensive examination of the effect of inclusion shape on the stiffness of two-phase linear and non-linear composites. To do so, we consider inclusions which are prolate or oblate spheroids, as indicated in Fig. 1, and we examine the full range of inclusion shapes from thin disk-like inclusions to slender needle-like inclusions. Attention is focused on inclusions which are stiffer than the matrix material, and a wide range of contrasts in phase moduli is examined in order to fully discern the role of inclusion shape on the stiffness of binary systems.

In the case of linearly elastic constituents, both phases are assumed to be isotropic and incompressible. Exact constitutive relations are developed for dilute concentrations of inclusions, and these are used in conjunction with a differential self-consistent scheme to obtain approximate constitutive relations applicable at higher concentrations of inclusions. The results for linear composites then form the basis for obtaining constitutive relations for incompressible, non-linear two-phase composites. The method used to make the extension to non-linear matrix behavior was developed by Ponte Castaneda (1991) and is based on a variational procedure. In his study, Ponte Castaneda obtained estimates for the constitutive behavior of non-linear matrix materials containing spherical voids or inclusions. In this work, we use it to obtain rigorous bounds on the constitutive behavior of power-law matrix materials containing a dilute concentration of aligned or randomly oriented rigid spheroidal inclusions, as well as to obtain estimates for the constitutive behavior of these two-phase systems when the concentration of inclusions exceeds dilute levels. In order to assess the accuracy of the constitutive relations obtained with the variational procedure, the results obtained for aligned inclusions are contrasted with accurate results presented by Lee and Mear (1991).

In the analysis, use is made of constitutive potentials rather than working directly with the tensorial components of stress and strain. The potential employed is the potential of the stress, ϕ, defined such that $\varepsilon = \partial\phi/\partial\sigma$. The potentials for the materials comprising the matrix and the inclusions are denoted as ϕ_m and ϕ_I, respectively, and the behavior of the two constituents are fully characterized in terms of these potentials. The specific forms of the potentials for linearly elastic material behavior and for non-linear matrix behavior will be specified further below.

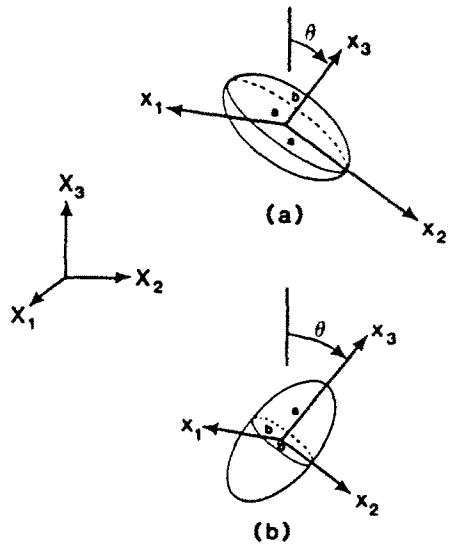

Fig. 1. Schematics of oblate inclusion with major semi-axes of length a and minor semi-axes of length b (a) and prolate inclusion with major semi-axis of length a and minor semi-axes of length b (b). Coordinate system $\{X_1, X_2, X_3\}$ is a fixed reference frame, and $\{x_1, x_2, x_3\}$ is a local coordinate system with the x_3 axis directed along the axis of symmetry of the inclusion.

To describe the behavior of the composite in terms of the potentials for the constituents, consider a representative block of material which has volume V_r and which contains a distribution of spheroidal inclusions. Let S_r denote the outer surface of the block, and assume that tractions $\boldsymbol{\Sigma}\cdot\mathbf{n}$ are prescribed on S_r, where $\mathbf{n}$ is the outwardly directed unit normal to the surface and $\boldsymbol{\Sigma}$ is the macroscopic stress tensor. The macroscopic strain $\mathbf{E}$ is given in terms of the displacement $\mathbf{u}$ on S_r by (Hill, 1967)

$$\mathbf{E} = \frac{1}{2V_r}\int_{S_r} (\mathbf{u}\otimes\mathbf{n}+\mathbf{n}\otimes\mathbf{u})\,dS \tag{1}$$

and the potential for the composite Φ, which has the property that $\mathbf{E} = \partial\Phi/\partial\boldsymbol{\Sigma}$, is given by

$$\Phi(\boldsymbol{\Sigma}) = \frac{1}{V_r}\int_{V_r} \phi\,dV. \tag{2}$$

In this relation, $\phi = \phi_m$ in the portion of the volume occupied by the matrix and $\phi = \phi_I$ in the remainder of the volume.

The behavior of the composite is known once the potential for the composite Φ has been determined. The quantity which is required in order to estimate this potential is the change in $\int_V \phi\,dV$ resulting from the introduction of a single inclusion into an unbounded region of the matrix material subject to a prescribed uniform remote stress $\boldsymbol{\Sigma}$. It is fairly evident that this is the quantity which is required to establish the macroscopic potential when the concentration of inclusions is dilute. In this case the inclusions do not interact, and the contribution from each inclusion contained in V_r can be established by treating the inclusion as if it were isolated (see, e.g., Budiansky and O'Connell, 1976; Duva and Hutchinson, 1984). Estimates of the composite properties for non-dilute concentration of inclusions can also be made based on this quantity through the use of a self-consistent method, as discussed further below.

Thus, an essential step in the analysis is the determination of the change in $\int_V \phi\,dV$ associated with the introduction of an isolated inclusion into an unbounded region of the matrix material. For the case of linear constituents, this quantity will be determined using Eshelby's (1957) equivalent inclusion method. Estimates for the moduli of the linear composites will then be constructed, and the role of inclusion shape on the stiffness of the two-phase isotropic and transversely isotropic composites will be examined. For non-linear matrix behavior, the accurate solution of the kernel problem for an isolated inclusion is very difficult. Lee and Mear (1991) have recently solved the non-linear kernel problem for cases of axisymmetric deformation (in which the axis of symmetry of the inclusion is aligned with the axis of symmetry of the loading), but results for arbitrary loading (or, equivalently, arbitrary orientation of the inclusion) are not presently available. In this work, we treat general loading/orientation by means of an approximate construction which avoids the need for the explicit solution of the kernel problem. The procedure will be discussed after constitutive relations have been established for linearly elastic composites.

2. LINEARLY ELASTIC COMPOSITES

In this section, we consider two-phase composites comprised of linearly elastic, isotropic and incompressible constituents. We assume that the shear modulus for the inclusions, G_I, is larger than the shear modulus for the matrix material, G_m, so that the inclusions serve as stiffening agents. As mentioned above, the analysis will be carried out in terms of constitutive potentials rather than working directly with the tensorial components of stress and strain. The potential of the stress which characterizes the matrix material is the (complementary) strain energy density function,

$$\phi_m(\boldsymbol{\sigma}) = \frac{1}{6G_m}\sigma_e^2, \tag{3}$$

where $\sigma_e = (3\boldsymbol{\sigma}' : \boldsymbol{\sigma}'/2)^{1/2}$ is the effective stress and $\boldsymbol{\sigma}'$ is the stress deviator. The potential of the stress for the inclusion material is given by (3) with G_m replaced by G_I.

The inclusions are assumed to be prolate or oblate spheroids with major semi-axis (or axes) of length a and minor semi-axis (or axes) of length b, as shown in Fig. 1. The shape of the inclusions is described by the aspect ratio $\xi \equiv a/b$, which ranges from one (corresponding to a spherical inclusion) to infinity.

In the development to follow, use will be made of two Cartesian coordinate systems. The $\{X_1, X_2, X_3\}$ system indicated in Fig. 1 will serve as a fixed reference frame, and the $\{x_1, x_2, x_3\}$ system will be a local frame attached to an inclusion. In this local frame, the x_3 axis is directed along the axis of symmetry of the inclusion, and the orientation of the x_1 and x_2 axes will be specified further below in a way which proves particularly convenient for the analysis.

2.1. *Structure of constitutive relations*

As already emphasized, the quantity which is needed in order to estimate the potential for a composite containing a dispersion of spheroids is the change in $\int_V \phi \, dV$ resulting from the introduction of a single inclusion into an infinite region of the matrix material. For a single inclusion of unit volume, we *denote* this quantity as $\delta\Phi/\delta c$ and, for a fixed remote stress state $\boldsymbol{\Sigma}$, it depends on the aspect ratio of the inclusion, the orientation of the inclusion with respect to the reference frame, and the moduli G_m and G_I. The structure of the macroscopic potential in terms of this quantity will be established in the remainder of this section, and in Section 2.2 the solution of the kernel problem for an isolated inclusion will be obtained using Eshelby's equivalent inclusion method. The structure of the constitutive relation for isotropic composites is discussed first, after which the form of the constitutive relation for transversely isotropic composites is presented.

2.1.1. *Randomly oriented inclusions.* Consider first the case of a matrix material containing a dilute concentration of randomly oriented spheroidal inclusions of a given aspect ratio, as shown schematically in Fig. 2a. The potential for the composite is

$$\Phi(\boldsymbol{\Sigma}) = \phi_m(\boldsymbol{\Sigma}) + c\left\langle \frac{\delta\Phi}{\delta c} \right\rangle \tag{4}$$

where $\langle \delta\Phi/\delta c \rangle$ denotes the average of $\delta\Phi/\delta c$ over all possible orientations, and c is the volume fraction of inclusions. Note that the quantity $c\langle \delta\Phi/\delta c \rangle$ represents the change in macroscopic potential for a dilute dispersion of spheroids of a given aspect ratio, whether or not the inclusions each have the same volume (provided, of course, that the distribution of inclusions is such that the composite material is macroscopically homogeneous).

Since the inclusions are randomly oriented and the phases are incompressible, the overall response of the composite is isotropic and completely characterized by a single shear modulus for the composite, $\bar{G}$. The potential for the composite takes the form

$$\Phi(\boldsymbol{\Sigma}) = \frac{1}{6G_m}\Sigma_e^2 + c\left\langle \frac{\delta\Phi}{\delta c} \right\rangle \equiv \frac{1}{6\bar{G}}\Sigma_e^2 \tag{5}$$

where Σ_e is the macroscopic effective stress. The quantity $\langle \delta\Phi/\delta c \rangle$ can be expressed as

$$\left\langle \frac{\delta\Phi}{\delta c} \right\rangle = -\frac{g}{6G_m}\Sigma_e^2 \tag{6}$$

where the function $g = g(\xi, \Gamma)$ depends on the aspect ratio of the reference inclusion and

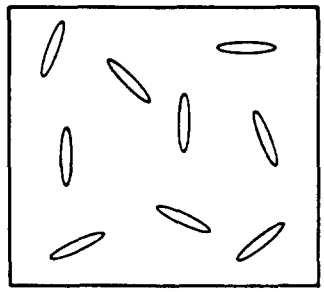

(a)

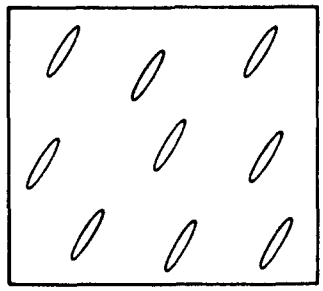

(b)

Fig. 2. Schematic of composite in which second phase inclusions are randomly oriented (a) and aligned (b). In case (a) the composite is macroscopically homogeneous and isotropic, while in case (b) it is macroscopically homogeneous and transversely isotropic.

the contrast in phase moduli $\Gamma \equiv G_I/G_m$, but not upon the remote loading. It must be determined through the solution of a boundary value problem for an (arbitrarily oriented) isolated inclusion followed by a suitable averaging over all orientations of the inclusion; details will be given in Section 2.2. The shear modulus for a composite in which the concentration of inclusions is dilute is then given by

$$\frac{G_m}{\tilde{G}} = 1 - cg. \tag{7}$$

The dilute limit neglects interaction between inclusions, so that its validity is limited to small volume fractions c. To obtain an approximation for $\tilde{G}$ which is valid over a larger range of inclusion concentrations, we employ the differential self-consistent scheme described by McLaughlin (1977).

Toward developing a differential self-consistent estimate for $\tilde{G}$, consider increasing the inclusion concentration by a differential amount while retaining the same remote loading. The resulting increment in Φ is

$$d\Phi = -\frac{1}{6\tilde{G}^2}\Sigma_e^2\, d\tilde{G}. \tag{8}$$

According to the differential self-consistent scheme, $d\Phi$ can also be evaluated using $\langle \delta\Phi/\delta c \rangle$ for the introduction of a differential amount of the second phase into an infinite region of matrix material *with properties of the composite* at the current stress level Σ_e. The corresponding change in Φ is estimated as

$$d\Phi = \frac{1}{(1-c)}\left\langle\frac{\delta\Phi}{\delta c}\right\rangle dc = -\frac{1}{(1-c)}\frac{g}{6\bar{G}}\Sigma_e^2\,dc \tag{9}$$

where (6) has been used with G_m replaced by $\bar{G}$. The term $(1-c)$ is included to account, in an approximate way, for the fact that a portion of the material replaced under the operation was already associated with the second phase (see McLaughlin, 1977). Combining (8) and (9) leads to a simple differential equation for $\bar{G}$ which can be integrated directly to obtain

$$\frac{G_m}{\bar{G}} = (1-c)^q. \tag{10}$$

The constant arising during the integration has been determined from the condition that $\lim_{c\to 0}\bar{G} = G_m$. Note that both the dilute and differential self-consistent approximations are fully specified once g is known. The determination of this function is discussed in Section 2.2 after the structure of the constitutive relation for the aligned inclusions has been developed.

2.1.2. *Aligned inclusions.* Now consider inclusions which are aligned as shown schematically in Fig. 2b, and which are distributed in such a way that the composite is (macroscopically) transversely isotropic. As mentioned above, the x_3 axis of the local coordinate system $\{x_1, x_2, x_3\}$ is directed along the axis of symmetry of the inclusion. The direction of x_1 within the median plane can be chosen freely, and it will emerge that the most convenient choice for it is such that the in-plane normal stress components in this local system are equal. That is, if $\{\mathbf{e}_1, \mathbf{e}_2, \mathbf{e}_3\}$ are the unit base vectors along the coordinate directions, then we choose x_1 such that $\Sigma_{11} = \Sigma_{22}$ where $\Sigma_{11} = \mathbf{e}_1\cdot\Sigma\cdot\mathbf{e}_1$ and $\Sigma_{22} = \mathbf{e}_2\cdot\Sigma\cdot\mathbf{e}_2$. It is always possible to determine the direction of $\mathbf{e}_1$ relative to the fixed coordinate system such that this condition is met.

The macroscopic potential can be expressed in the form

$$\Phi(\Sigma) = \frac{1}{2\bar{E}_a}\Sigma_a^2 + \frac{1}{6\bar{G}_{ip}}\Sigma_{ip}^2 + \frac{1}{6\bar{G}_{op}}\Sigma_{op}^2 \tag{11}$$

where $\bar{E}_a$, $\bar{G}_{ip}$ and $\bar{G}_{op}$ are three moduli which completely describe the behavior of the composite, and the stress quantities which appear are given in terms of the components of the macroscopic stress tensor in the *local coordinate system* as (also see Appendix A)

$$\Sigma_a^2 = (\Sigma_{33}-\Sigma_{11})^2, \quad \Sigma_{ip}^2 = 3\Sigma_{12}^2, \quad \Sigma_{op}^2 = 3(\Sigma_{13}^2+\Sigma_{23}^2). \tag{12}$$

These quantities can be interpreted as effective stresses associated with the axisymmetric stress state $\{\Sigma_{11} = \Sigma_{22}, \Sigma_{33}\}$, the in-plane shear stress Σ_{12}, and the out-of-plane shear stresses $\{\Sigma_{13}, \Sigma_{23}\}$, respectively. The modulus $\bar{E}_a$ is Young's modulus for uniaxial stressing along the x_3-direction, $\bar{G}_{ip}$ is a shear modulus representing the response of the solid to in-plane shear stress Σ_{12}, and $\bar{G}_{op}$ is a shear modulus associated with the out-of-plane shear stresses Σ_{13} and Σ_{23}.

The change in $\int_V \phi\,dV$ resulting from the introduction of a single inclusion of unit volume into an unbounded region of the matrix material can be expressed similarly:

$$\frac{\delta\Phi}{\delta c} = -\frac{g_a}{6G_m}\Sigma_a^2 - \frac{g_{ip}}{6G_m}\Sigma_{ip}^2 - \frac{g_{op}}{6G_m}\Sigma_{op}^2. \tag{13}$$

Once the functions $g_a = g_a(\xi, \Gamma)$, $g_{ip} = g_{ip}(\xi, \Gamma)$ and $g_{op} = g_{op}(\xi, \Gamma)$ have been established, the potential for a composite containing a dilute dispersion of aligned inclusions can be computed as

$$\Phi(\Sigma) = \phi_m(\Sigma) + c\frac{\delta\Phi}{\delta c} \tag{14}$$

and the three moduli for the composite determined from

$$\frac{3G_m}{\bar{E}_a} = 1 - cg_a, \quad \frac{G_m}{\bar{G}_{ip}} = 1 - cg_{ip}, \quad \frac{G_m}{\bar{G}_{op}} = 1 - cg_{op}. \tag{15a,b,c}$$

The determination of the functions g_a, g_{ip} and g_{op} will be taken up in the next section.

Estimates for the moduli of composites in which the concentration of inclusions exceeds dilute levels can be obtained using a self-consistent scheme which utilizes the solution for an isolated inclusion in a transversely isotropic matrix material. The resulting estimates are quite cumbersome (e.g. McLaughlin, 1977), and here we choose instead to develop simple relations for moduli by employing the solution to the kernel problem for an *isotropic* matrix in conjunction with the differential self-consistent scheme. The method is applied separately to determine each of the three moduli. This is done by considering purely axisymmetric loading (in the local coordinate frame) to find $\bar{E}_a$, a stress state consisting of only in-plane shear to determine $\bar{G}_{ip}$ and, finally, a stress state in which only out-of-plane shear stresses act in order to establish $\bar{G}_{op}$. Establishing the moduli in this way is possible because the three separate modes of deformation considered in determining them are fully uncoupled. The results of the calculations are

$$\frac{3G_m}{\bar{E}_a} = (1-c)^{q_a}, \quad \frac{G_m}{\bar{G}_{ip}} = (1-c)^{q_{ip}}, \quad \frac{G_m}{\bar{G}_{op}} = (1-c)^{q_{op}} \tag{16a,b,c}$$

and it is easily verified that these relations reduce to (15) for dilute inclusion volume fractions. For large volume fractions, the relations (16) are only estimates of the moduli, and no attempt has been made here to assess the range of volume fractions for which they provide an accurate characterization of the composite material. Such an assessment would necessarily involve direct numerical calculations of the moduli for non-dilute (e.g. periodic) distributions of inclusions.

The effective moduli for the transversely isotropic composite containing aligned spheroidal inclusions can be estimated once the functions g_a, g_{ip} and g_{op} have been established. This is similar to the case of the isotropic composite in which only the function g remained unknown. These functions depend on the aspect ratio of the inclusions and the modulus contrast Γ, but not upon the remote loading. They are most readily established using Eshelby's equivalent inclusion method, as discussed next.

2.2. *Determination of g-functions*

In the previous section, the forms for the macroscopic potential and moduli for an incompressible linearly elastic matrix strengthened by a dispersion of randomly oriented spheroidal inclusions or by a dispersion of aligned inclusions was established. In the former case, there was a single scalar function g which remained to be determined, and for the transversely isotropic composite there were three functions g_a, g_{ip} and g_{op} which required specification. To determine these functions, a boundary value problem must be solved for a single oblate or prolate spheroidal inclusion of unit volume and aspect ratio ξ embedded in an infinite region of matrix material. This is most readily carried out using Eshelby's equivalent inclusion method. We review the method in the context of the current problem, and then we discuss the calculation of the g-functions.

To apply Eshelby's method, first consider an infinite region of the matrix material which is free of a physical inhomogeneity and absent of external loading. Imagine that the region V_I (which an inhomogeneity would occupy if it were present) is allowed to undergo an unconstrained transformation strain ε^T. The corresponding constrained strain within V_I is uniform and given by $\varepsilon^c = \mathbf{S} : \varepsilon^T$ where $\mathbf{S}$ is Eshelby's tensor. Imagine now that a remote stress Σ with deviator Σ' is also present. Then the total strain within V_I is $\varepsilon^{\text{total}} = (\mathbf{E} + \varepsilon^c)$

where $\mathbf{E} = \boldsymbol{\Sigma}'/(2G_m)$. The objective is to choose the transformation strain such that the total strain and the stress (deviator) within V_I are precisely what they would be within the inhomogeneity were it present. Denote the actual strain within the physical inhomogeneity as $\boldsymbol{\varepsilon}^I$. Then the transformation strain must be selected such that $\boldsymbol{\varepsilon}^{\text{total}} = \boldsymbol{\varepsilon}^I$ and $G_m[\boldsymbol{\varepsilon}^{\text{total}} - \boldsymbol{\varepsilon}^T] = G_I\boldsymbol{\varepsilon}^I$, where the term in the brackets is the elastic part of the strain $\boldsymbol{\varepsilon}^{\text{total}}$. Combining these two conditions, and using Eshelby's tensor to relate the constrained strain to the transformation strain, we obtain

$$[(\Gamma-1)\mathbf{S}+\mathbf{I}]:\boldsymbol{\varepsilon}^T = -(\Gamma-1)\mathbf{E} \tag{17}$$

where Γ is the modulus contrast defined previously and $\mathbf{I}$ is the fourth order identity tensor. The components of Eshelby's tensor are known in terms of elementary functions for spheroidal regions V_I; the values relevant to the current investigation are listed in Appendix A in terms of ξ.

To affect the inversion of (17), first consider the component associated with E_{33}, where the indices indicate components relative to the local coordinate system $\{x_1, x_2, x_3\}$:

$$(\Gamma-1)S_{33ij}\varepsilon_{ij}^T + \varepsilon_{33}^T = -(\Gamma-1)E_{33}. \tag{18}$$

Now, because the coordinate system has been selected such that $\Sigma_{11} = \Sigma_{22}$, and because the constituents are incompressible, it follows that $\varepsilon_{33}^T = -2\varepsilon_{22}^T = -2\varepsilon_{11}^T$ [this can be seen directly through inspection of (17) along with the properties of S]. We then obtain

$$\varepsilon_{33}^T = \frac{(\Gamma-1)E_{33}}{(\Gamma-1)(S_{3311}-S_{1111})-1} \tag{19a}$$

where the property that $S_{3311} = S_{3322}$ has been used.

Next, consider the equations associated with E_{12}, E_{13} and E_{23}. The equations involve only the transformation strains ε_{12}^T, ε_{13}^T and ε_{23}^T, respectively (i.e. they are not coupled with other components of $\boldsymbol{\varepsilon}^T$, except those which are equal by symmetry of the tensor) so that we immediately obtain

$$\varepsilon_{12}^T = \frac{(\Gamma-1)E_{12}}{2(1-\Gamma)S_{1212}-1}, \quad \varepsilon_{13}^T = \frac{(\Gamma-1)E_{13}}{2(1-\Gamma)S_{1313}-1}, \quad \varepsilon_{23}^T = \frac{(\Gamma-1)E_{23}}{2(1-\Gamma)S_{2323}-1}. \tag{19b,c,d}$$

Now that the transformation strain has been determined in terms of the macroscopic strain (or, equivalently, the macroscopic stress deviator), the change in $\int_V \phi \, dV$ due to the introduction of the single inclusion of unit volume into the infinite block of matrix material can be calculated as (Eshelby, 1957)

$$\frac{\delta\Phi}{\delta c} = \tfrac{1}{2}\boldsymbol{\varepsilon}^T:\boldsymbol{\Sigma}. \tag{20}$$

To use this relation to calculate g_a, consider an axisymmetric stress state $\{\Sigma_{11} = \Sigma_{22}, \Sigma_{33}\}$. It then follows from (13), (19a) and (20) that

$$g_a(\xi,\Gamma) = \frac{(\Gamma-1)}{(\Gamma-1)(S_{3311}-S_{3333})-1}. \tag{21}$$

Similarly, we obtain

$$g_{ip}(\xi,\Gamma)=\frac{(\Gamma-1)}{2(1-\Gamma)S_{1212}-1} \tag{22}$$

and

$$g_{op}(\xi,\Gamma)=\frac{(\Gamma-1)}{2(1-\Gamma)S_{2323}-1}. \tag{23}$$

The components of Eshelby's tensor which enter into these expressions depend upon whether the inclusion is a prolate or oblate spheroid and upon the aspect ratio ξ (see Appendix A).

This completes the specification for the composite containing aligned inclusions. For the composite containing randomly oriented inclusions, the function g must be obtained by a suitable averaging over all possible orientations of an inclusion. Because the constitutive potential for this case, eqn (5), depends only on the effective stress, it is sufficient to consider a single macroscopic stress state. A convenient choice is uniaxial tension. Let T be the level of uniaxial stress assumed to be directed along the X_3 axis of the fixed reference coordinate system. For this stress state, the single angle θ between the X_3-axis and the x_3-axis (see Fig. 1) suffices to specify the orientation of the inclusion. An average over all possible orientations of the inclusion then takes the simple form

$$\langle\cdot\rangle=\int_0^{\pi/2}(\cdot)\sin\theta\,\mathrm{d}\theta. \tag{24}$$

Now, the components of $\Sigma=T\mathbf{i}_3\otimes\mathbf{i}_3$ in the local coordinate system (with x_1 chosen as specified above) can be expressed in terms of the angle θ and the tensile stress T, and the results inserted into (13) to obtain

$$\frac{\delta\Phi}{\delta c}=-\frac{T^2}{96G_m}\{(3\cos 2\theta+1)^2g_a+12g_{ip}\sin^4\theta+12g_{op}\sin^2 2\theta\}. \tag{25}$$

Then, by carrying out the average indicated by (24) and noting that (25) depends only on the effective stress which, for uniaxial tension, is $\Sigma_e=T$, we obtain

$$g=\tfrac{1}{5}(g_a+2g_{ip}+2g_{op}). \tag{26}$$

Note that for the special case of spherical inclusions, $g=g_a=g_{ip}=g_{op}$. This follows since the sphere has no preferred orientation and the change in $\int_V\phi\,\mathrm{d}V$ depends only on the effective stress Σ_e.

2.3. *Effect of inclusion shape on stiffness*

Constitutive relations have been established for composite materials comprised of linearly elastic, isotropic and incompressible constituents in which the second phase consists of spheroidal inclusions. Both isotropic composites (containing randomly oriented inclusions) and transversely isotropic composites (containing aligned inclusions) have been treated. In this section we use these constitutive relations to examine the role that inclusion shape plays in the resulting stiffness of the composite material. Composites in which the inclusions are randomly oriented are examined first, followed by an examination of transversely isotropic composites.

2.3.1. *Randomly oriented inclusions.* Consider first a dilute concentration of randomly oriented inclusions. A measure of the stiffening effect of the inclusions is the change in the

constitutive potential due to the presence of the inclusions (i.e. the change in strain energy), $\Delta\Phi = \Phi - \phi(\Sigma)$, which is given by

$$\Delta\Phi = -cg\frac{1}{6G_m}\Sigma_e^2. \tag{27}$$

Since $\Delta\Phi$ is negative, the larger the magnitude of this quantity, the larger the stiffening effect of the inclusions.

Now, let the composite containing a dilute concentration of spherical inclusions serve as a reference to which other composites containing the *same* volume fraction of second phase will be compared, and let $\Delta\Phi_{sph}$ denote the change in potential for this reference composite. Then the ratio $\Delta\Phi/\Delta\Phi_{sph}$ represents the increase in stiffness resulting from a given dilute volume fraction of non-spherical inclusions relative to the increase in stiffness resulting from the same volume fraction of spherical inclusions. This quantity can be expressed in terms of the shear modulus for the composite containing non-spherical inclusions, $\bar{G}$, and the shear modulus for the composite containing spherical inclusions, $\bar{G}_{sph}$, as

$$\frac{\Delta\Phi}{\Delta\Phi_{sph}} = \frac{1 - G_m/\bar{G}}{1 - G_m/\bar{G}_{sph}} \tag{28}$$

and is plotted in Fig. 3 as a function of the contrast in phase moduli for several inclusion aspect ratios.

From the figure it is evident that, for a given inclusion concentration and contrast in phase moduli, the larger the aspect ratio of the inclusions, the stiffer is the composite. It is also evident that the *degree* to which the shape of the second phase inclusions affects the composite stiffness depends strongly on the contrast in phase moduli. For example, when $\Gamma = 2$, oblate inclusions with an aspect ratio of 100:1 give rise to an increase in stiffness which is approximately 10% greater than the corresponding increase in stiffness achieved with spherical inclusions. Whereas, when $\Gamma = 10$, oblate inclusions with an aspect ratio of 100:1 result in an increase in stiffness exceeding two and a half times that achieved with spherical inclusions.

Over the entire range of aspect ratios and contrasts in phase moduli displayed in Fig. 3, a greater increase in stiffness is achieved with oblate inclusions than with prolate inclusions

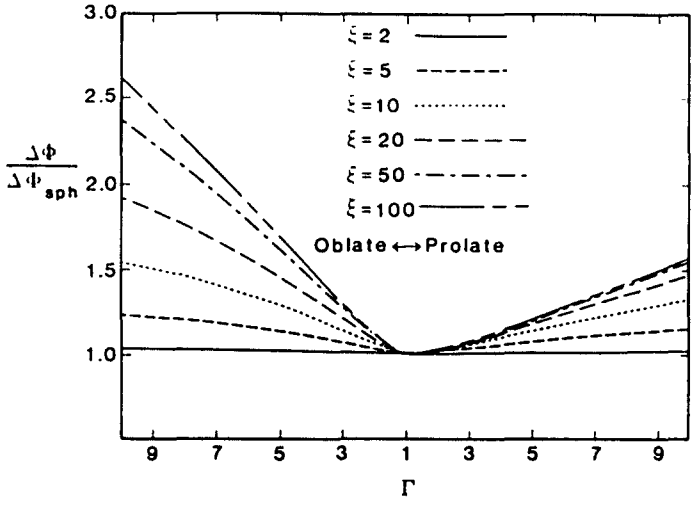

Fig. 3. Change in constitutive potential resulting from randomly oriented inclusions, $\Delta\Phi = \Phi - \phi$, normalized by change in potential resulting from spherical inclusions, $\Delta\Phi_{sph}$, as a function of contrast in phase moduli Γ. Comparison made at the same (arbitrary) dilute volume fraction of inclusions, and for several aspect ratios ξ. Values of $\Delta\Phi/\Delta\Phi_{sph}$ greater than one indicate that the composite is stiffer than it would be if inclusions were spherical rather than spheroidal.

when the comparison is made at the same aspect ratio. For larger contrasts in phase moduli, however, there may exist a range of aspect ratios for which prolate inclusions are to be preferred as stiffening agents, as can be seen from the results shown in Fig. 4. In the latter figure, $\Delta\Phi/\Delta\Phi_{sph}$ is presented as a function of ξ for several values of Γ. Note that for $\Gamma = (100, \infty)$, there does in fact exist a range of aspect ratios (dependent upon Γ) over which prolate inclusions provide more stiffening than do oblate inclusions.

A careful examination of the behavior of $\Delta\Phi/\Delta\Phi_{sph}$ as a function of aspect ratio and contrast in phase moduli reveals that for $\Gamma < 66.8$, oblate inclusions are always to be preferred to prolate inclusions as stiffening agents when the comparison is made at the same aspect ratio. When $\Gamma = 66.8$, however, prolate and oblate inclusions with aspect ratio $\xi \approx 18$ give rise to the same increase in stiffness, and for contrast in phase moduli $\Gamma > 66.8$, there exists a range of aspect ratios, say $\xi_l < \xi < \xi_u$, over which prolate inclusions give rise to more stiffening than do oblate inclusions. As a particular example, consider again the case $\Gamma = 100$ displayed in Fig. 4. In this case, it is found that the lower and upper limits of the range of aspect ratios over which prolate inclusions are to be preferred to oblate inclusions as stiffening agents are $\xi_l \approx 10.5$ and $\xi_u \approx 48$, respectively. It is also found that the aspect ratio for which the most benefit is to be gained from prolate inclusions relative to that to be gained from oblate inclusions is $\xi \approx 29$, and that the corresponding value of $\Delta\Phi/\Delta\Phi_{sph}$ for prolate inclusions is approximately 37% larger than that for oblate inclusions. More generally, it is found that the larger the contrast in phase moduli, the larger is the difference $(\xi_u - \xi_l)$, and the larger is the maximum (positive) difference between $\Delta\Phi/\Delta\Phi_{sph}$ for prolate and oblate inclusions. Indeed, as Γ ranges from $\Gamma = 66.8$ to $\Gamma = \infty$, the value of ξ_l decreases monotonically from $\xi_l = 18$ to $\xi_l = 7.5$, the value of ξ_u increases monotonically from $\xi_u = 18$ to $\xi_u = \infty$, and the maximum increase in stiffness to be gained from prolate inclusions relative to that to be gained from oblate inclusions increases monotonically from zero to infinity.

Now consider the differential self-consistent estimate for the shear modulus of the composite given by (10). The estimate for $G_m/\tilde{G}$ is shown in Fig. 5a–d, as a function of aspect ratio and volume fraction, for $\Gamma = (5, 10, 100, \infty)$. Note that the results displayed in these figures represent the total stiffening effect of the second phase inclusions, and not the effect relative to a composite containing spherical inclusions.

When $\Gamma = 5$ and the volume concentration is 5% (Fig. 5a), oblate inclusions with an aspect ratio of 100:1 result in a composite shear modulus of $\tilde{G}/G_m = 1.14$, while spherical inclusions lead to $\tilde{G}/G_m = 1.08$. In this instance, the ratio of the *increase* in shear modulus resulting from the oblate inclusions to that achieved with spherical inclusions is 1.75. When the volume concentration is increased to 20%, oblate inclusions with an aspect ratio of 100:1 and spherical inclusions give rise to $\tilde{G}/G_m = 1.78$ and $\tilde{G}/G_m = 1.41$, respectively. At

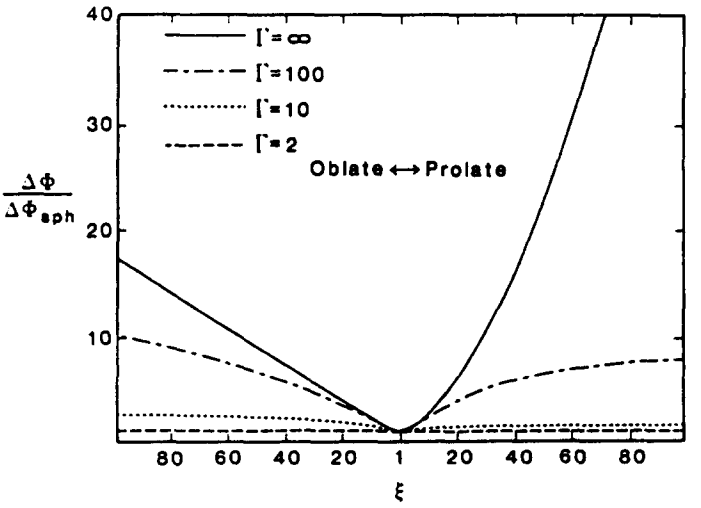

Fig. 4. Ratio $\Delta\Phi/\Delta\Phi_{sph}$ for randomly oriented inclusions, as a function of aspect ratio ξ and modulus contrast Γ.

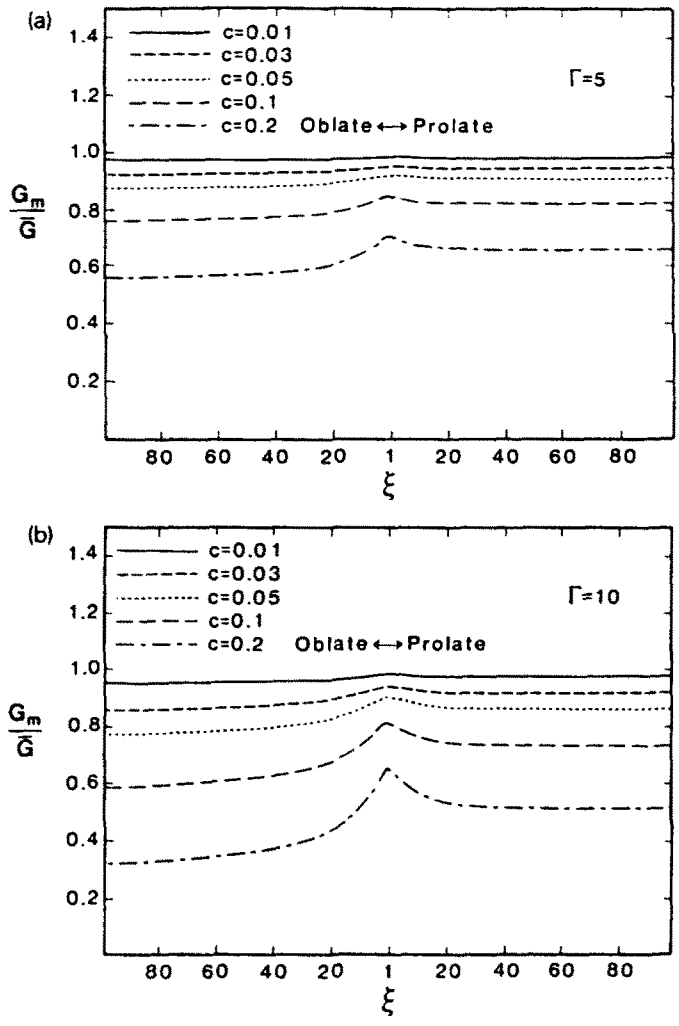

Fig. 5. (a), (b) Differential self-consistent estimate of $G_m/\bar{G}$ given by (10), as a function of aspect ratio ξ and volume fraction of inclusions for $\Gamma = 5$ (a) and $\Gamma = 10$ (b).

this larger volume fraction, the ratio of the increase in shear modulus resulting from the oblate inclusions to that achieved with spherical inclusions is 1.95. Thus, the effect that the shape of the inclusions has on the stiffness of the composite is enhanced by an increase in the volume fraction of the inclusions.

From the results shown in Fig. 5a–d, it is clear that the effect of inclusion shape on the stiffness of the composite is more pronounced as Γ is increased, as has already been noted for dilute concentrations of inclusions. At a fixed volume fraction of inclusions and a fixed contrast in phase moduli, the larger the aspect ratio, the greater is the stiffness of the composite. As a specific example, consider $\Gamma = 10$ and a volume fraction of 20%. From Fig. 5b it is seen that thin disk-shaped oblate inclusions with aspect ratio 100:1 give rise to 103% more stiffening than do spherical inclusions, whereas slender needle-like prolate inclusions with this same aspect ratio give rise to 29% more stiffening than do spherical inclusions. From the figures, it is also seen that for the modest moduli contrasts of $\Gamma = (5, 10)$, oblate inclusions are to be preferred as stiffening agents, while for the moduli contrasts of $\Gamma = (100, \infty)$ there is a range of aspect ratios for which prolate inclusions are to be preferred as stiffening agents. In fact, it follows from the structure of the estimate (10) that this range of aspect ratios is identical to that for dilute concentrations of inclusions.

2.3.2. *Aligned inclusions.* We now examine the behavior of composites containing aligned inclusions. The composites are transversely isotropic and incompressible, and hence three moduli are required to fully characterize their multiaxial stress–strain response. The

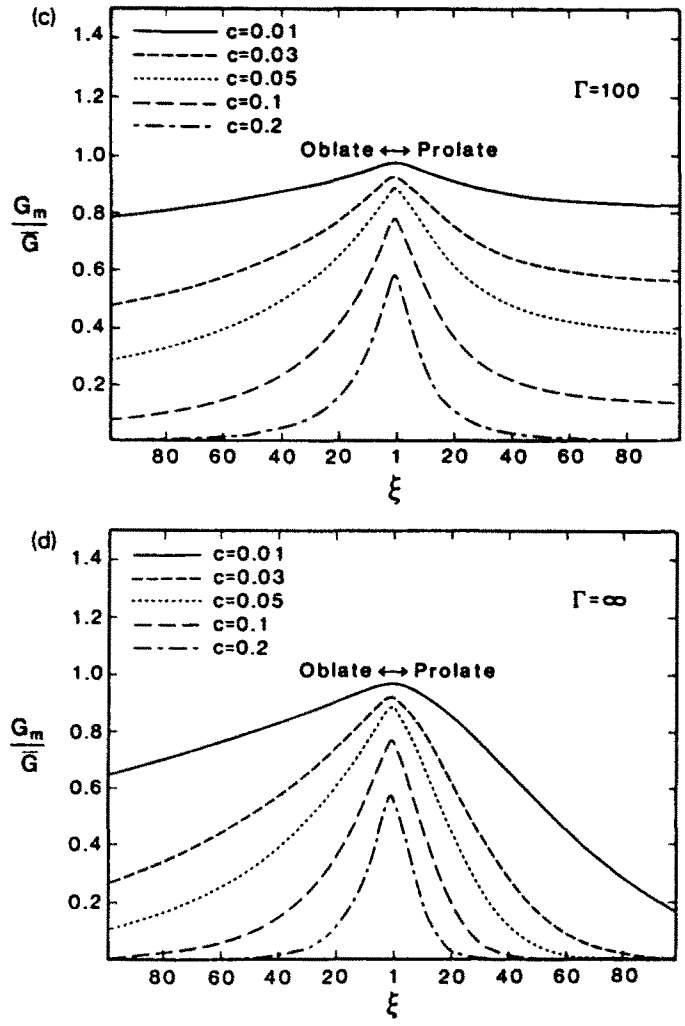

Fig. 5. (c), (d) Differential self-consistent estimate of $G_m/\bar{G}$ given by (10), as a function of aspect ratio ξ and volume fraction of inclusions for $\Gamma = 100$ (c) and $\Gamma = \infty$ (d).

moduli which have been introduced are a Young's modulus $\bar{E}_a$ associated with uniaxial tension along the direction of alignment of the inclusions (i.e. along the x_3-axis), and two shear moduli $\bar{G}_{ip}$ and $\bar{G}_{op}$ associated with in-plane shearing and out-of-plane shearing, respectively. For dilute concentrations of inclusions these moduli are given by (15), and estimates for them when the concentration is non-dilute are given by (16). In this section we examine how each of these moduli are affected by the shape of the second phase inclusions. Since the predictions are qualitatively similar for dilute and non-dilute concentrations of inclusions, only results for dilute concentrations will be presented.

To explore the effect of inclusion shape on the axial Young's modulus $\bar{E}_a$, consider axisymmetric deformation of the composite with the symmetry axis of the loading parallel to the x_3-axis. As for the case of randomly oriented inclusions, it is convenient to examine the ratio $\Delta\Phi/\Delta\Phi_{sph}$ (in which $\Delta\Phi$ and $\Delta\Phi_{sph}$ are computed at the same dilute volume concentration) since this quantity is independent of c. In Fig. 6 this ratio is displayed as a function of modulus contrast $\Gamma \leqslant 10$ for several aspect ratios, and in Fig. 7 it is displayed for several modulus contrasts as a function of aspect ratio. It is apparent from these figures that, for the range of modulus contrasts and aspect ratios considered, prolate inclusions are always more potent stiffening agents than are oblate inclusions when the comparison is made at the same aspect ratio. This is, in fact, the case for the full range of aspect ratios and any contrast in phase moduli exceeding unity. From the figures, it is also apparent that the difference between the stiffening achieved with prolate inclusions and that achieved with oblate inclusions becomes more pronounced as the modulus contrast is increased.

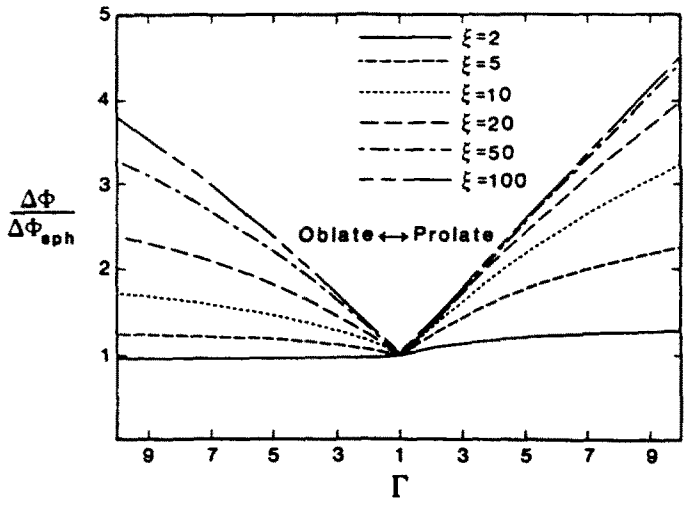

Fig. 6. Ratio $\Delta\Phi/\Delta\Phi_{sph}$ for aligned inclusions and axisymmetric loading, as a function of modulus contrast Γ and aspect ratio ξ.

To examine the effect of inclusion shape on the in-plane shear modulus $\tilde{G}_{ip}$, consider in-plane shearing of the composite (i.e. assume that the only component of stress acting in the local $\{x_1, x_2, x_3\}$ coordinate frame is Σ_{12}). For this loading, the difference between the behavior for oblate inclusions and for prolate inclusions is dramatic, as can be seen from Fig. 8. This figure displays $\Delta\Phi/\Delta\Phi_{sph}$ computed for dilute concentrations of inclusions. It is clear that only oblate inclusions provide stiffening which exceeds that achieved with spherical inclusions, and the greatest increase in the resistance to in-plane shearing is achieved with thin oblate inclusion. Note also that for prolate inclusions, there is little sensitivity of the in-plane shear modulus to the shape of the inclusions when the aspect ratio exceeds $\xi \approx 5$.

Finally, we examine the effect of inclusion shape on the out-of-plane shear modulus $\tilde{G}_{op}$. To do so, we consider out-of-plane shearing of the composite in which the only non-zero components of stress acting are Σ_{13} and Σ_{23}. Results for $\Delta\Phi/\Delta\Phi_{sph}$ computed at dilute concentrations of inclusions are shown in Fig. 9. It is apparent from the figure that, in general, the larger the aspect ratio of the inclusions, the less effective they are in increasing the out-of-plane shear modulus above that for the pure matrix material. An exception is that prolate inclusions with $1 < \xi < 2$ are actually somewhat more effective in reinforcing

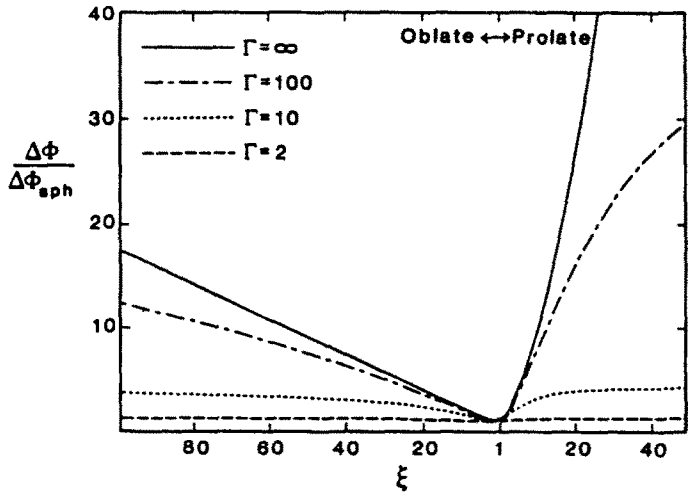

Fig. 7. Ratio $\Delta\Phi/\Delta\Phi_{sph}$ for aligned inclusions and axisymmetric loading, as a function of aspect ratio ξ and modulus contrast Γ.

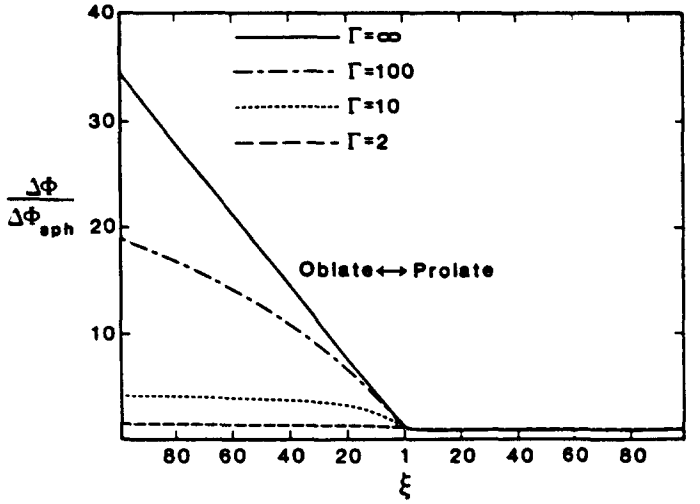

Fig. 8. Ratio $\Delta\Phi/\Delta\Phi_{sph}$ for aligned inclusions and in-plane shearing, as a function of aspect ratio ξ and modulus contrast Γ.

against this mode of deformation than are spherical inclusions. For example, when $\Gamma = 10$, the most effective inclusion shape is prolate with $\xi = 1.39$, and such inclusions lead to a stiffening which is 1.8% greater than that achieved with the same volume fraction of spheres. It can also be seen from the figure that the ratio of the stiffening provided by non-spherical inclusions to that provided by spherical inclusions decreases as the ratio of phase moduli increases, and that at a given aspect ratio the stiffening provided by oblate inclusions is less than that provided by prolate inclusions.

3. NON-LINEAR MATRIX BEHAVIOR

The constitutive relations presented above are restricted to linearly elastic composites. Applications of two-phase composites often involve plastic deformation or creep of the matrix, and in this section we extend the constitutive theory to account for such behavior. Attention is respected to composites comprised of a pure power-law matrix material reinforced by rigid spheroidal inclusions. Approximate constitutive relations are obtained for both randomly oriented inclusions and for aligned inclusions by using a procedure proposed by Ponte Castaneda (1991). The resulting approximate constitutive relations are

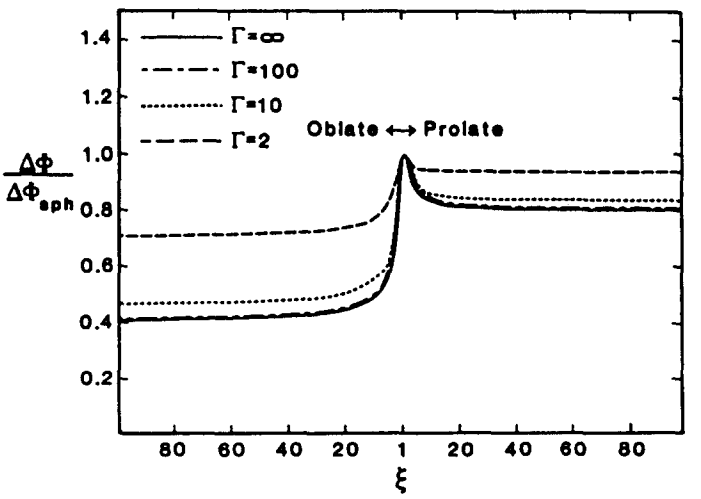

Fig. 9. Ratio $\Delta\Phi/\Delta\Phi_{sph}$ for aligned inclusions and out-of-plane shearing, as a function of aspect ratio ξ and modulus contrast Γ.

then assessed, at least in a limited way, by comparing predictions for the axisymmetric deformation of a composite containing aligned inclusions with accurate results for this case recently obtained by Lee and Mear (1991).

3.1. *Description of matrix material and composite*

The uniaxial stress–strain behavior of the matrix material is modeled using the pure power-law relation $\varepsilon/\varepsilon_0 = (\sigma/\sigma_0)^n$ where σ_0 and ε_0 are a reference stress and strain, respectively. This constitutive relation embodies a full range of matrix behavior, from the incompressible linearly elastic material considered in Section 2 (for $n = 1$) to a rigid–perfectly plastic matrix (as $n \to \infty$). The multi-axial behavior of the matrix material is described by

$$\frac{\boldsymbol{\varepsilon}}{\varepsilon_0} = \frac{3}{2}\left(\frac{\sigma_e}{\sigma_0}\right)^{n-1}\frac{\boldsymbol{\sigma}'}{\sigma_0} \tag{29}$$

which is the J_2-deformation theory generalization of the uniaxial behavior. The potential of the stress corresponding to (29), defined such that $\boldsymbol{\varepsilon} = \partial\phi/\partial\boldsymbol{\sigma}$, is

$$\phi(\boldsymbol{\sigma}) = \frac{\varepsilon_0\sigma_0}{n+1}\left(\frac{\sigma_e}{\sigma_0}\right)^{n+1}. \tag{30}$$

We note that while the analysis will be carried out in terms of the non-linear hyperelastic relation (29), the results also apply to a non-linear viscous matrix material when strain quantities are reinterpreted as strain-rate quantities. In this case, the constitutive relation is a prototype for a material undergoing steady state creep.

To characterize the behavior of the composite material, we again consider a representative block of volume V, which contains a distribution of spheroidal inclusions. The outer surface of the block, S, is subjected to tractions $\boldsymbol{\Sigma}\cdot\mathbf{n}$ where $\boldsymbol{\Sigma}$ is the macroscopic stress, and the corresponding macroscopic strain is defined in terms of the resulting displacements on S, by (1). As for the linear case, we choose to work in terms of the potential for the composite rather than the tensorial components of stress and strain, and this potential is given in terms of the local potential distribution by (2). Because the inclusions are assumed to be rigid, the integral over the volume can be replaced by an integral over the volume of the matrix V_m.

Toward establishing an approximation for the macroscopic potential Φ, consider the complementary minimum principle for deformation theory introduced by Hill (1956). For our current application, the functional on which the principle is based can be expressed in the form

$$\mathscr{P}(\boldsymbol{\sigma}^*) = \int_{V_m} \phi(\boldsymbol{\sigma}^*)\,\mathrm{d}V \tag{31}$$

where $\boldsymbol{\sigma}^*(\mathbf{x})$ is any statically admissible stress field. The actual stress field is distinguished from all other admissible fields in that it renders $\mathscr{P}$ its minimal value. It follows that an upper bound on the macroscopic potential is given by

$$\Phi^*(\boldsymbol{\Sigma}) = \frac{1}{V}\mathscr{P}(\boldsymbol{\sigma}^*) \tag{32}$$

and that the actual macroscopic potential satisfies

$$\Phi = \inf_{\boldsymbol{\sigma}^*}\Phi^*. \tag{33}$$

Estimates for Φ could be constructed (numerically) by considering a class of admissible

stress fields (i.e. trial functions) and seeking a minimum to $\mathscr{P}$ over these trial functions. An estimate for Φ would then be given by $\mathscr{P}^*_{\min}/V$, where $\mathscr{P}^*_{\min}$ denotes the minimum with respect to the trial functions considered and is greater than or equal to the true minimum $\mathscr{P}_{\min}$. Ponte Castaneda's method differs from such a procedure in that it does not require that trial functions be explicitly constructed. Instead, it requires only that a solution for a linearly elastic matrix containing the same distribution of inclusions be known. In what follows, we summarize the procedure for the case of current interest (see also the discussion given in Appendix B); a more general discussion with applications to other types of constituent behavior is given by Ponte Castaneda (1991).

3.2. *Construction of approximate constitutive relations*

To develop the procedure, assume that the solution for a *comparison* composite comprised of a linearly elastic matrix with (as yet arbitrary) shear modulus G_c is known, and denote the potential for the linear matrix as $\phi_c = \sigma_e^2/(6G_c)$. If we introduce a function ψ according to

$$\phi(\boldsymbol{\sigma}) = \phi_c(\boldsymbol{\sigma}) - \psi(\boldsymbol{\sigma}), \tag{34}$$

then it follows that

$$\Phi(\boldsymbol{\Sigma}) = \inf_{\boldsymbol{\sigma}^*} \frac{1}{V_r} \int_{V_m} \{\phi_c(\boldsymbol{\sigma}^*) - \psi(\boldsymbol{\sigma}^*)\}\, \mathrm{d}V. \tag{35}$$

Although the integrand appearing in this latter relation is unknown, a bound on Φ can be obtained rather easily by replacing $\psi(\boldsymbol{\sigma})$ with the constant ψ_-, given by

$$\psi_- = \sup_{\boldsymbol{\sigma}} \{\phi_c(\boldsymbol{\sigma}) - \phi(\boldsymbol{\sigma})\} \tag{36}$$

$$= \frac{1}{6G_c} \frac{(n-1)}{(n+1)} \left(\frac{\sigma_0^n}{3\varepsilon_0 G_c}\right)^{2/(n-1)} \tag{37}$$

where the explicit forms for the potentials ϕ_c and ϕ have been used. There then results

$$\Phi \geqslant \Phi_c - (1-c)\psi_- \tag{38}$$

where Φ_c is the macroscopic potential for the comparison composite which is known (by assumption). Thus, a *lower* bound for Φ can be obtained for any given $G_c > 0$, and we now seek the best such bound as

$$\Phi \geqslant \sup_{G_c > 0} \{\Phi_c - (1-c)\psi_-\} \equiv \Phi_{glb}. \tag{39}$$

To solve the optimization problem (39), it is convenient to first write $\Phi_c = \tilde{\Phi}_c/(6G_c)$ where $\tilde{\Phi}_c$ depends upon the macroscopic stress and the concentration, shape and distribution of the rigid inclusions, but is independent of the shear modulus for the comparison matrix material. Then, upon inserting the expression for ψ_- given by (37) into (39) and carrying out the indicated operation, there results

$$\Phi_{glb} = \frac{\varepsilon_0 \sigma_0}{n+1} \frac{1}{(1-c)^{(n-1)/2}} \left(\frac{\tilde{\Phi}_c}{\sigma_0^2}\right)^{(n+1)/2}. \tag{40}$$

Using this relation, a bound on the constitutive potential for a composite comprised of rigid inclusions and a pure power-law matrix material (30) can be obtained, provided that the exact constitutive potential for a linearly elastic matrix containing an equivalent

distribution of rigid inclusions is known. If only an estimate for $\tilde{\Phi}_c$ is available, then (40) can only provide an estimate (rather than a bound) on the behavior of the non-linear composite. In what follows, the constitutive potentials established in Section 2 for linear composites are used in conjunction with (40) to provide approximate constitutive potentials for non-linear composites in which the inclusions are randomly oriented or aligned.

3.2.1. *Randomly oriented inclusions.* Consider first randomly oriented rigid inclusions, and assume that the inclusion spacing is such that the concentration can be considered dilute *when the matrix is elastic.* The macroscopic potential for a linear matrix is given exactly by (5) and (7), from which it follows that $\tilde{\Phi}_c = (1-cg)\Sigma_e^2$ where $g = g(\xi, \infty)$ is given by (26). Inserting $\tilde{\Phi}_c$ into (40), it is then found that

$$\Phi_{glb} = E_0 \frac{\sigma_0}{n+1}\left(\frac{\Sigma_e}{\sigma_0}\right)^{n+1} \tag{41}$$

where E_0 is a reference strain for the composite (not to be confused with a Young's modulus) given by

$$\frac{E_0}{\varepsilon_0} = \frac{(1-cg)^{(n+1)/2}}{(1-c)^{(n-1)/2}}. \tag{42}$$

If the inclusion spacing is such that their interaction can be ignored for the non-linear matrix as well as for the linear matrix, then it is appropriate to expand (42) for small c and retain only the terms which are linear in c. This results in a dilute approximation for the non-linear composite given by

$$\frac{E_0}{\varepsilon_0} = 1 - ch_{lub} \tag{43}$$

where

$$h_{lub} = \frac{(n+1)}{2}g - \frac{(n-1)}{2}. \tag{44}$$

Unfortunately, the procedure outlined above cannot be used to establish rigorous bounds on the behavior of non-linear composites when the concentration of inclusions exceeds dilute values (i.e. dilute for the elastic matrix). This is because only estimates are available for $\tilde{\Phi}_c$ rather than exact results. Nonetheless, *estimates* for Φ applicable for non-dilute concentrations can be easily constructed. One way to construct such estimates is to use the bound for the dilute theory (43) in conjunction with the differential self-consistent scheme outlined in Section 2 (see also Lee and Mear, 1991). The procedure is essentially the same as for a linear matrix, and the resulting potential function for non-dilute concentrations has the form (41), with

$$E_0 = \varepsilon_0(1-c)^{h_{lub}}. \tag{45}$$

An alternative procedure is to start with the differential self-consistent estimate (10) for which $\tilde{\Phi}_c = (1-c)^q\Sigma_e^2$, and to then use (40) to obtain an estimate for the non-linear matrix. The potential function obtained from this latter calculation is identical to the potential obtained with the first procedure.

The composite reference strain for non-dilute concentration of inclusions, eqn (45), is shown in Fig. 10 as a function of aspect ratio for several volume fractions and two hardening exponents. These approximate results for the reference strain indicate that, except for aspect ratios in the range $1 < \xi < 7.5$, prolate inclusions are to be preferred to oblate inclusions as stiffening agents. This is the same conclusion that was drawn for randomly oriented rigid inclusions in a linear matrix [as expected from the form of (44)]. The results also predict that the stiffening which results from a fixed volume fraction of inclusions is a strong function of matrix non-linearity; the stiffness of the composite relative to the matrix material is much greater for a highly non-linear matrix material than for a linear matrix material.

3.2.2. *Aligned inclusions.* Consider now inclusions which are aligned and concentrations which are sufficiently small so that interactions between inclusions are negligible when the matrix is linear. In this case [see (11) and (15)]

$$\tilde{\Phi}_c = [1 - cg_a]\Sigma_a^2 + [1 - cg_{ip}]\Sigma_{ip}^2 + [1 - cg_{op}]\Sigma_{op}^2 \tag{46}$$

so that

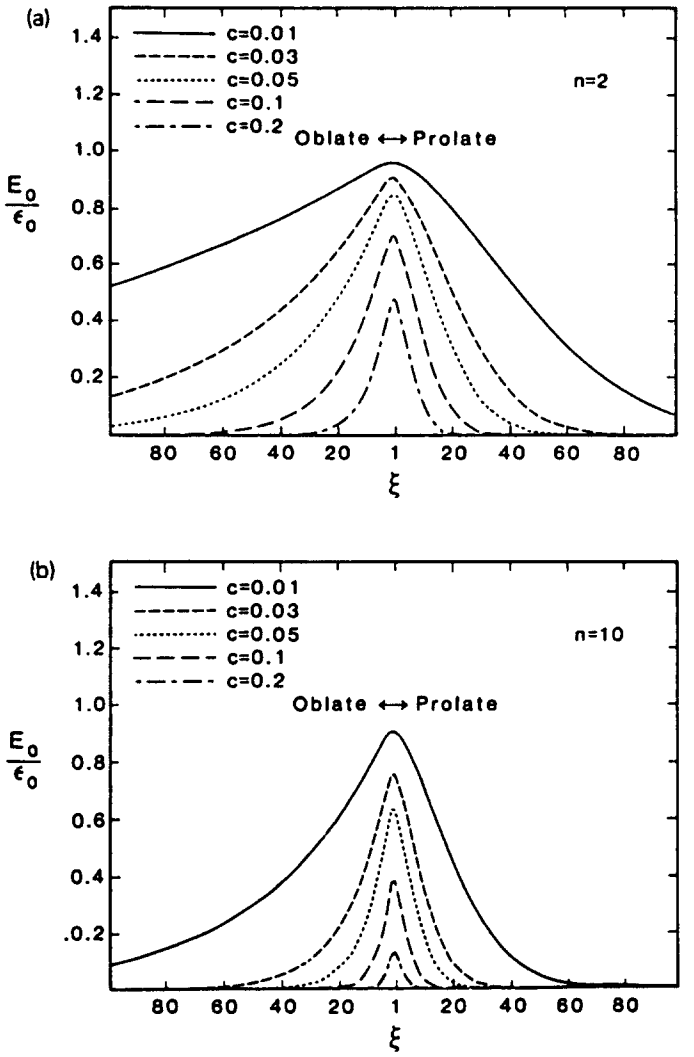

Fig. 10. Composite reference strain for randomly oriented rigid inclusions, E_0, as a function of aspect ratio ξ and volume fraction of inclusions for $n = 2$ (a) and $n = 10$ (b).

$$\Phi_{qlh} = (1-c)^{(1-n)/2}\left\{1-c\left[g_a\left(\frac{\Sigma_a}{\Sigma_e}\right)^2+g_{ip}\left(\frac{\Sigma_{ip}}{\Sigma_e}\right)^2+g_{op}\left(\frac{\Sigma_{op}}{\Sigma_e}\right)^2\right]\right\}^{(n+1)/2}\phi(\Sigma_e) \tag{47}$$

where we have used $\Sigma_e^2 = \Sigma_a^2+\Sigma_{ip}^2+\Sigma_{op}^2$, and where

$$\phi(\Sigma_e) = \frac{\varepsilon_0\sigma_0}{n+1}\left(\frac{\Sigma_e}{\sigma_0}\right)^{n+1}. \tag{48}$$

The functions g_a, g_{ip} and g_{op} which appear in these relations are given by (21), (22) and (23), respectively, with $\Gamma \to \infty$. For future reference, we note that the quantity $\Delta\Phi/\Delta\Phi_{sph}$ plotted in Fig. 7 is equivalent to g_a/g_{sph} where $g_{sph} = g(1, \Gamma)$, and that Figs 8 and 9 can similarly be interpreted as plots of g_{ip}/g_{sph} and g_{op}/g_{sph}. We also note that for rigid inclusions $g_{sph} = 2.5$.

Now, if the inclusions concentration is dilute for the non-linear matrix as well as for the linear matrix, then it is appropriate to expand (47) in powers of c and retain only the terms which are linear in c. This results in a dilute theory for the non-linear composite given by

$$\Phi_{qlh} = \left\{1+c\frac{(n-1)}{2}-c\frac{(n+1)}{2}\left[g_a\left(\frac{\Sigma_a}{\Sigma_e}\right)^2+g_{ip}\left(\frac{\Sigma_{ip}}{\Sigma_e}\right)^2+g_{op}\left(\frac{\Sigma_{op}}{\Sigma_e}\right)^2\right]\right\}\phi(\Sigma_e). \tag{49}$$

For the special case of axisymmetric loading (with the axis of loading oriented in the direction of inclusion alignment), the dilute theory for the non-linear composite specializes to

$$\Phi_{qlh} = (1-ch^a_{lah})\frac{\varepsilon_0\sigma_0}{n+1}\left(\frac{\Sigma_a}{\sigma_0}\right)^{n+1} \tag{50}$$

where

$$h^a_{lah} = \frac{(n+1)}{2}g_a-\frac{(n-1)}{2}. \tag{51}$$

It is apparent that the stiffening predicted to result from a dilute concentration of inclusions is qualitatively the same for non-linear and linear matrix materials. Specifically (see behavior of g_a shown in Fig. 7), it is predicted that prolate inclusions provide more stiffening than do oblate inclusions when the comparison is made at a fixed aspect ratio and volume concentration of inclusions. Similarly, an examination of the approximate constitutive relation (49) specialized to in-plane or out-of-plane shearing reveals that the effect of inclusion shape on the stiffening is qualitatively the same for non-linear and linear matrix materials. Of course, the magnitude of the stiffening provided by a given concentration of inclusions depends strongly upon the degree of matrix non-linearity.

Finally, for concentration of inclusions which cannot be considered dilute for a linear matrix, an estimate for the constitutive potential can be obtained by using the estimates for the linear composite moduli given by (16). Forming $\tilde{\Phi}_c$ for this case and using (40), it is found that

$$\Phi_{est} = (1-c)^{(1-n)/2}\left\{(1-c)^{g_a}\left(\frac{\Sigma_a}{\Sigma_e}\right)^2+(1-c)^{g_{ip}}\left(\frac{\Sigma_{ip}}{\Sigma_e}\right)^2+(1-c)^{g_{op}}\left(\frac{\Sigma_{op}}{\Sigma_e}\right)^2\right\}^{(n+1)/2}\phi(\Sigma_e). \tag{52}$$

For the special case of axisymmetric loading, this relation specializes to

$$\Phi_{est} = (1-c)^{h^a_{lub}} \frac{\varepsilon_0 \sigma_0}{n+1} \left(\frac{\Sigma_a}{\sigma_0}\right)^{n+1} \tag{53}$$

and again it is predicted that prolate inclusions are to be preferred to oblate inclusions as a means to stiffen the matrix material against axial deformation. Note that the effect of the inclusions on the axial stiffness of the composite is predicted to be a strong function of matrix non-linearity, and that the greater the non-linearity, the greater is the stiffening provided by the inclusions.

3.2.3. *Evaluation of approximate constitutive relations.* The approximate constitutive potentials for rigid inclusions in a power-law matrix material have been obtained using only information about the constitutive behavior for linearly elastic composites. Since the flow fields for an inclusion (or inclusions) in a non-linear matrix is expected to differ substantially from the corresponding fields for a linear matrix, the accuracy of the approximations is suspect, particularly for large hardening exponents. To make an assessment of the accuracy of results obtained with Ponte Castaneda's procedure, we now focus our attention on the axisymmetric loading of a non-linear matrix stiffened by aligned rigid spheroidal inclusions. For this case, accurate results for a dilute concentration of inclusions have recently been obtained by Lee and Mear (1991), allowing a direct evaluation of the corresponding predictions obtained above to be made. Lee and Mear also constructed differential self-consistent estimates for non-dilute concentrations of inclusions, but we will consider only the dilute limit where Ponte Castaneda's procedure is known to give a lower bound for Φ.

In their study, Lee and Mear modeled the behavior of the matrix material with the multiaxial relation (29) and considered a wide range of shapes of rigid inclusion from oblate with an aspect ratio of 100 : 1 to prolate with an aspect ratio of 50 : 1. It was demonstrated that the potential for the composite has the form

$$\Phi = E^a_0 \frac{\sigma_0}{n+1} \left(\frac{\Sigma_a}{\sigma_0}\right)^{n+1} \tag{54}$$

where $E^a_0 = E^a_0(\xi, n, c)$ is a reference strain for the composite and $\Sigma_a = |\Sigma_{33} - \Sigma_{11}|$ is the macroscopic effective stress. The reference strain is given by

$$E^a_0 = \varepsilon_0(1 - ch_a) \tag{55}$$

where $h_a = h_a(\xi, n)$ is a function which depends on the aspect ratio of the inclusions and the hardening exponent, but not upon the remote loading.

The determination of the function h_a requires the solution of a boundary value problem for an isolated inclusion in the non-linear matrix. The solution to this kernel problem was obtained using a spectral method based on Hill's (1956) functional of the displacements, as modified by Budiansky *et al.* (1982) to render it applicable for infinite domains. In this procedure, trial displacement functions were obtained using a displacement potential in spheroidal coordinates, and a set of unknown coefficients appearing in the trial functions was determined by minimizing the functional. Details are given in Lee and Mear (1991). The values for h_a obtained with the procedure are upper bounds and are believed to be accurate to within approximately 1%.

From (50), a lower bound on the reference strain is found to be given by

$$E^a_0 = \varepsilon_0(1 - ch^a_{lub}) \tag{56}$$

where h^a_{lub} is given by (51). To compare h^a_{lub} with the function h_a obtained by Lee and Mear, it is convenient to first scale them by

$$\beta \equiv \begin{cases} \left(\frac{b}{a}\right)^2, & \text{for prolate inclusions.} \\ \left(\frac{b}{a}\right), & \text{for oblate inclusions.} \end{cases} \tag{57}$$

The function β corresponds to the volume of an inclusion for which $a = a^* = (3/4\pi)^{1/3}$, and the functions $\tilde{h}_a \equiv \beta h_a$ and $\tilde{h}^a_{lub} \equiv \beta h^a_{lub}$ can be interpreted as being associated with inclusions of this fixed dimension a^* rather than inclusions of unit volume. The scaled functions are convenient because they remain bounded in the limit $\xi \to \infty$ (see also Lee and Mear, 1991).

The functions $\tilde{h}_a$ and $\tilde{h}^a_{lub}$ are plotted in Fig. 11a for $n = 2$ and in Fig. 11b for $n = 10$. As can be seen, the accuracy of the bound deteriorates as the amount of matrix non-linearity increases. This should be expected from the nature of the approximations involved in the construction of the estimate. For spherical inclusions and $n = 2$, the estimates obtained using Ponte Castaneda's method differ from the accurate estimates by 15%, while for spherical inclusions and $n = 10$ the difference is 55%. When $n = 10$ and the inclusions are prolate with large aspect ratios, the estimates obtained with Ponte Castaneda's procedure are in error by more than 200%.

Duva (1984) has developed constitutive relations for a pure power law matrix (29) stiffened by rigid spherical inclusions. His procedure is essentially that followed by Lee and Mear (1991), and for dilute concentrations of inclusions and axisymmetric loading he arrived at the constitutive relation (50) and (51) with $g = g(1, \infty) = 2.5$. To extend his

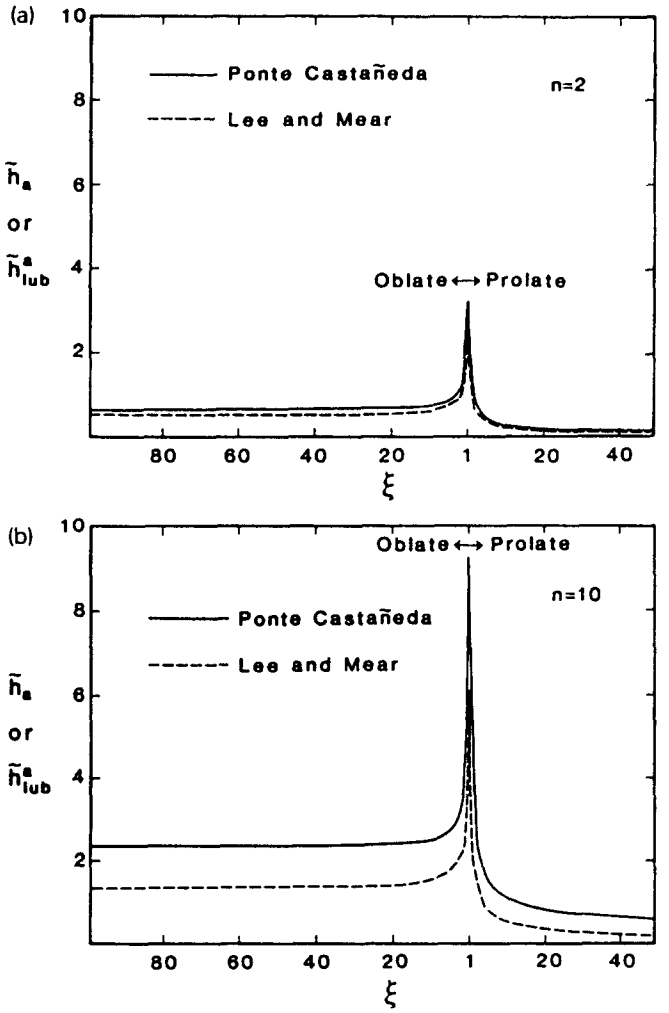

Fig. 11. Functions $\tilde{h}_a = \beta h_a$ and $\tilde{h}^a_{lub} = \beta h^a_{lub}$ vs aspect ratio ξ for $n = 2$ (a) and $n = 10$ (b).

constitutive theory to arbitrary remote stressing, he proposed that the influence of the third invariant of Σ' be neglected and that the potential (50) be retained with Σ_a simply replaced by Σ_e. Note that Ponte Castaneda's (1991) procedure applied to spherical inclusions (or more generally, to randomly oriented inclusions) gives rise to a constitutive potential which is also a function of the effective stress only. This functional dependence on the stress is imposed on the approximate constitutive potential by the use of a linear comparison solid (Appendix B), yet a dependence on the third invariant of the macroscopic stress deviator cannot be rule out *a priori*.

The accuracy of the estimate for spherical inclusions obtained with Ponte Castaneda's method has already been discussed for axisymmetric loading. If the influence of the third invariant of the stress deviator is in fact negligible for this case, then the inaccuracy of the approximate constitutive relations (41) and (43) for general loading is the same as for axisymmetric loading. In particular, the accuracy of the predictions deteriorates rapidly with increasing hardening exponent. Now, while accurate results are not currently available for the constitutive behavior of non-linear composites comprised of randomly oriented spheroidal inclusions, it should be expected that the accuracy of the approximate relations for these cases will also deteriorate with increasing non-linearity. In addition, it is likely that, as for aligned inclusions, the severity of the error will increase with increasing aspect ratio.

4. CONCLUSIONS

Explicit constitutive relations have been established for incompressible, linear and non-linear two-phase composites. The second phase has been assumed to be comprised of spheroidal inclusions, and aligned inclusions (giving rise to a transversely isotropic composite) as well as randomly oriented inclusions (giving rise to an isotropic composite) have been treated.

The constitutive theories developed for both linear and non-linear composites are valid over the full range of aspect ratios, and have been used to explore the effect of inclusion shape on the stiffness of two-phase composites. Attention has been restricted to cases in which the stiffness of the second phase exceeds that of the primary phase (so that the inclusions act as stiffening agents), and results have been presented for both dilute and non-dilute concentrations of inclusions. We first summarize the findings for linear composites, and then we discuss the extensions to non-linear matrix behavior.

For isotropic linearly elastic composites, it has been demonstrated that when the ratio of the shear modulus for the inclusions to the shear modulus for the matrix is less than 66.8, oblate inclusions are always more effective stiffening agents than are prolate inclusions when the comparison is made at the same aspect ratio. When the contrast in phase moduli exceeds 66.8, however, there is a range of aspect ratios for which prolate inclusions are to be preferred as stiffening agents. For example, when the shear modulus of the inclusions is 100 times that of the matrix material, this range of inclusion aspect ratios is approximately $11 < \xi < 48$. As the contrast in phase moduli increases, the range of aspect ratios over which prolate inclusions are to be preferred as stiffening agents also increases, and as the mathematical limit of a rigid second phase is approached, the range of aspect ratios for which prolate inclusions are the preferred stiffening agent is $7.5 < \xi < \infty$.

For transversely isotropic linearly elastic composites, the behavior is more complicated because there are three independent moduli which are affected by the shape of the inclusions. The moduli used to describe the behavior of the transversely isotropic composite are a Young's modulus $\bar{E}_a$ associated with uniaxial tension along the direction of alignment of the inclusions (i.e. along the x_3-axis shown in Fig. 1), a shear modulus $\bar{G}_{ip}$ associated with shearing in the x_1–x_2 plane, and a shear modulus $\bar{G}_{op}$ associated with shearing in the x_1–x_3 and x_2–x_3 planes.

It has been found that prolate inclusions are always to be preferred to oblate inclusions as a means to increase the axial Young's modulus $\bar{E}_a$, with the degree of sensitivity to the shape of the inclusions dependent on the contrast in phase moduli. The in-plane shear modulus $\bar{G}_{ip}$, on the other hand, is enhanced by increasing the aspect ratio for oblate

inclusions but diminished by increasing the aspect ratio for prolate inclusions. The behavior of the out-of-plane shear modulus is different: it is greatest when the inclusions have small aspect ratios, and is significantly diminished by an increase in aspect ratio whether the inclusions are tending to become more oblate or more prolate. Clearly, tailoring a composite for increased resistance to one mode of deformation must be done with due regard to the fact that it may diminish its performance in resisting other modes of deformation.

The extension of the constitutive relations to account for non-linear matrix behavior has been carried out using a procedure proposed by Ponte Castaneda (1991). This procedure exploits the solution to the kernel problem (i.e. the boundary value problem for an isolated inclusion) for a linear matrix material rather than relying on the solution of a non-linear kernel problem. Explicit constitutive relations have been established for power-law matrix materials containing rigid inclusions which are randomly oriented or aligned. When the concentration of inclusions is sufficiently small, the constitutive relations are rigorous bounds on the true behavior. For larger concentrations of inclusions this feature is lost, and the results can only be considered estimates of the actual constitutive behavior.

To assess the predictions obtained with Ponte Castaneda's scheme, results obtained for the axisymmetric deformation of composites comprised of a dilute concentration of rigid aligned inclusions have been contrasted with accurate results for this case presented by Lee and Mear (1991). This comparison indicates that Ponte Castaneda's scheme deteriorates as the hardening exponent is increased, with large errors occurring for $n = 10$. This is not surprising since only information for an inclusion in a linear matrix is used in the scheme. Even though an optimization is carried out on the (arbitrary) shear modulus of the linear comparison medium, it is not possible to capture the details of the flow field for an inclusion in a non-linear matrix.

At present, accurate results are not available for the constitutive behavior of composites when the second phase inclusions are randomly oriented. The constitutive relations obtained using Ponte Castaneda's procedure do give bounds (or estimates) on this behavior, but the comparisons made for the case of aligned inclusions causes the accuracy of these relations to be suspect. Development and evaluation of constitutive relations for randomly oriented and aligned elliptical inclusions in plane strain deformation are currently in progress, and it is expected that these studies will provide additional qualitative information about the accuracy of constitutive theories developed using Ponte Castaneda's method.

Finally, we remark that the constitutive relations developed for linear composites apply for all contrasts in phase moduli (except for the limiting case of a vacuous second phase) so that the effect of inclusions which are softer than the matrix material on the constitutive behavior could also be examined. In addition, Ponte Castaneda's method can be used for elastic inclusions (see Ponte Castaneda, 1991) in order to develop constitutive relations for deformable inclusions in a non-linear matrix material.

Acknowledgements—A grant from the ALCOA Foundation was used to support this work. We would like to thank Rich Becker and Greg Rodin for providing helpful comments throughout the course of this investigation.

REFERENCES

Budiansky, B. (1965). On the elastic moduli of some heterogeneous materials. *J. Mech. Phys. Solids* **13**, 223–227.
Budiansky, B. and O'Connell, R. J. (1976). Elastic moduli of a cracked solid. *Int. J. Solids Structures* **12**, 81–97.
Budiansky, B., Hutchinson, J. W. and Slutsky, S. (1982). Void growth and collapse in viscous solids. In *Mechanics of Solids* (Edited by H. G. Hopkins and M. J. Sewell), pp. 13–45. Pergamon Press, Oxford.
Duva, J. M. (1984). A self-consistent analysis of the stiffening effect of rigid inclusions on a power-law material. *J. Engng Mater. Technol.* **106**, 317–321.
Duva, J. M. and Hutchinson, J. W. (1984). Constitutive potentials for dilutely voided non-linear materials. *Mech. Mater.* **3**, 41–54.
Eshelby, J. D. (1957). The determination of the elastic field on an ellipsoidal inclusion and relatived problems. *Proc. R. Soc. Lond. A.* **241**, 376–396.
Hashin, Z. (1983). Analysis of composite materials—a survey. *J. Appl. Mech.* **50**, 481–505.
Hill, R. (1956). New horizons in the mechanics of solids. *J. Mech. Phys. Solids* **5**, 66–74.
Hill, R. (1965). A self-consistent mechanics of composite materials. *J. Mech. Phys. Solids* **13**, 213–222.
Hill, R. (1967). The essential structure of constitutive laws for metal composites and polycrystals. *J. Mech. Phys. Solids* **15**, 79–95.

Lee, B. J. and Mear, M. E. (1991). Effect of inclusion shape on the stiffness of non-linear two phase composites. *J. Mech. Phys. Solids* (in press).
McLaughlin, R. (1977). A study of the differential scheme for composite materials. *Int. J. Engng Sci.* **15**, 237–244.
Mori, T. and Tanaka, K. (1973). Average stress in the matrix and average elastic energy of materials with misfitting inclusions. *Acta Metall.* **21**, 571–574.
Ponte Castaneda, P. (1991). The effective mechanical properties of nonlinear isotropic composites. *J. Mech. Phys. Solids* **39**, 45–71.
Ponte Castaneda, P. and Willis, J. R. (1988). On the overall properties of nonlinearly viscous composites. *Proc. R. Soc. Lond. A* **416**, 217–244.
Qiu, Y. P. and Weng, G. J. (1990). The influence of inclusion shape on the overall elastoplastic behavior of two-phase isotropic composites. *Int. J. Solids Structures* **27**(12), 1537–1550.
Tandon, G. P. and Weng, G. J. (1984). The effect of aspect ratio of inclusions on the elastic properties of unidirectionally aligned composites. *Polymer Compos.* **5**, 327–333.
Tandon, G. P. and Weng, G. J. (1986). Average stress in the matrix and effective moduli of randomly oriented composites. *Comp. Sci. Technol.* **27**, 111–132.
Willis, J. R. (1983). The overall elastic response of composite materials. *J. Appl. Mech.* **50**, 1202–1209.
Wu, T. T. (1966). The effect of inclusion shape on the elastic moduli of a two-phase material. *Int. J. Solids Structures* **2**, 1–8.
Zhao, Y. H. and Weng, G. J. (1990). Theory of plasticity for a class of inclusion and fiber-reinforced composites. In *Micromechanics and Inhomogeneity* (Edited by G. J. Weng, M. Taya and H. Abe), pp. 599–622. Springer, New York.

APPENDIX A

Local coordinate system

Let $\{X_1, X_2, X_3\}$ be a fixed right handed Cartesian coordinate system, and let $\{x_1^*, x_2^*, x_3\}$ be a local right handed coordinate system attached to an inclusion with the x_3-axis directed along the axis of symmetry of the inclusion. The axes x_1^* and x_2^* lie within the median plane of the inclusion but are otherwise arbitrarily oriented. Consider a prescribed remote stress Σ and let Σ_{ij}^* denote the components of this stress tensor with respect to the $\{x_1^*, x_2^*, x_3\}$ system.

Now imagine rotating the $\{x_1^*, x_2^*\}$ axes about the x_3 axis in order to obtain a (special) coordinate system $\{x_1, x_2, x_3\}$ which is distinguished from all other systems (i.e. other orientations of x_1^*) in that in this new frame $\Sigma_{11} = \Sigma_{22}$. That is, if the unit base vectors for this new local coordinate system are $\{\mathbf{e}_1, \mathbf{e}_2, \mathbf{e}_3\}$, then we choose x_1 such that $\Sigma_{11} = \Sigma_{22}$ where $\Sigma_{11} = \mathbf{e}_1 \cdot \Sigma \cdot \mathbf{e}_1$ and $\Sigma_{22} = \mathbf{e}_2 \cdot \Sigma \cdot \mathbf{e}_2$.

For convenience, most of the analysis presented in this paper has been carried out in this local frame, but to apply the final results which have been obtained it is not necessary to actually determine the orientation of the x_1 axis. This is because only effective stress quantities are involved in the expression of the macroscopic potential (11), and only the components of the prescribed uniform remote stress in terms of *any* local coordinate system (x_1^*, x_2^*, x_3) need to be determined in order to evaluate these quantities. It is easily verified that

$$\Sigma_a^2 = \left(\Sigma_{11}^* - \frac{(\Sigma_{11}^* + \Sigma_{22}^*)}{2}\right)^2 \tag{A1}$$

$$\Sigma_{ap}^2 = 3[\tfrac{1}{4}(\Sigma_{11}^* - \Sigma_{22}^*)^2 + \Sigma_{12}^{*2}] \tag{A2}$$

and

$$\Sigma_{ap}^2 = 3(\Sigma_{13}^{*2} + \Sigma_{23}^{*2}) \tag{A3}$$

where, again, the Σ_{ij}^* denote the components of Σ in any coordinate system for which the x_3 axis is along the axis of the inclusions.

Eshelby's tensor

The components of Eshelby's tensor for spheroidal regions V_I can be expressed in terms of elementary functions and are given in Eshelby (1957). For an incompressible material, these components depend only upon whether the inclusion is a prolate or an oblate spheroid and upon the aspect ratio ξ. We list only terms which are relevant to the current application.

For prolate inclusions:

$$S_{3311} - S_{3333} = \frac{9\xi^2 - 3\xi(2\xi^2+1)(\xi^2-1)^{-1/2}\cosh^{-1}\xi}{2(\xi^2-1)^2} \tag{A4}$$

$$S_{1212} = \frac{1}{4} - \frac{1}{8(\xi^2-1)^2}\{2+\xi^2 - 3\xi(\xi^2-1)^{-1/2}\cosh^{-1}\xi\} \tag{A5}$$

$$S_{1313} = S_{2323} = \frac{(\xi^2+1)}{4(\xi^2-1)^2}\{2+\xi^2 - 3\xi(\xi^2-1)^{-1/2}\cosh^{-1}\xi\}. \tag{A6}$$

For oblate inclusions:

$$S_{3311}-S_{3333}=\frac{9\xi^2-3\xi^2(2\xi^2+1)(\xi^2-1)^{-1/2}\cos^{-1}\xi^{-1}}{2(\xi^2-1)^2} \tag{A7}$$

$$S_{1212}=\frac{1}{4}-\frac{\xi^2}{8(\xi^2-1)^2}\{1+2\xi^2-3\xi^2(\xi^2-1)^{-1/2}\cos^{-1}\xi^{-1}\} \tag{A8}$$

$$S_{1313}=S_{2323}=\frac{(\xi^2+1)}{4(\xi^2-1)^2}\{1+2\xi^2-3\xi^2(\xi^2-1)^{-1/2}\cos^{-1}\xi^{-1}\}. \tag{A9}$$

APPENDIX B

In this Appendix, a generalization of Ponte Castaneda's (1991) procedure for obtaining bounds (or estimates) for the effective properties of non-linear two-phase composites is given. While Ponte Castaneda's technique relies on a linear comparison solid (for which a macroscopic potential is assumed known), the generalization presented here begins with the assumption that the macroscopic potential is known for a non-linear comparison solid. This generalization has less practical utility than the original procedure, but forms the basis for discussion about the structure of the approximate constitutive relations and how this structure is tied to the structure of the comparison solid (rather than necessarily to the actual structure of the non-linear constitutive relation).

In the development, attention is restricted to power-law matrix materials (29) reinforced by a random distribution of rigid spheroidal inclusions, and the composites considered are assumed to be macroscopically homogeneous and isotropic. The macroscopic constitutive behavior for such composites can be described by a potential of the stress

$$\Phi=\frac{\varepsilon_0\sigma_0}{n+1}H(\Sigma/\sigma_0) \tag{B1}$$

where, for a given shape of the inclusion, the function H depends on the hardening exponent of the matrix material in addition to the macroscopic stress. In the following, we will use the notation Φ_n and H_n in place of Φ and H in order to explicitly indicate this dependence on the hardening exponent n. Since the composite is isotropic, H depends upon the stress only through the second and third invariants of the stress deviator Σ'. Further, since the matrix obeys the power-law relation (29) and the inclusions are rigid, H must be homogeneous of degree $(n+1)$ in the stresses.

Now, consider a (comparison) solid characterized by the potential

$$\phi_m=\frac{\varepsilon_c\sigma_0}{m+1}\left(\frac{\sigma_e}{\sigma_0}\right)^{m+1} \tag{B2}$$

where ε_c is a reference strain. The macroscopic potential for the non-linear comparison solid is given by

$$\Phi_m=\frac{\varepsilon_c\sigma_0}{m+1}H_m(\Sigma/\sigma_0) \tag{B3}$$

and we assume that H_m is known for the aspect ratio and distribution of inclusions of interest. What is sought is a bound on the potential of a composite which has the same morphology of the second phase but which is comprised of a matrix material governed by

$$\phi_n=\frac{\varepsilon_0\sigma_0}{n+1}\left(\frac{\sigma_e}{\sigma_0}\right)^{n+1}. \tag{B4}$$

Such a bound can be obtained following a procedure similar to that discussed in Section 3. Define $\psi\equiv\phi_m-\phi_n$, and then form

$$\psi_-=\sup_{\sigma_e}\psi=\varepsilon_0\sigma_0\frac{(n-m)}{(n+1)(m+1)}\left(\frac{\varepsilon_c}{\varepsilon_0}\right)^{(n+1)/(n-m)} \tag{B5}$$

where (B2) and (B4) have been used. It then follows that [see discussion near (38)]

$$\Phi_n\geq\Phi_m-(1-c)\psi_- \tag{B6}$$

and the best such bound is obtained by choosing $\varepsilon_c>0$ such that the right-hand side of the relation is maximized. The result of the calculation is

$$\Phi_n\geq\varepsilon_0\sigma_0\frac{1-c}{n+1}\left[\frac{H_m}{(1-c)}\right]^{(n+1)/(m+1)} \tag{B7}$$

and, by comparing this relation with (B1), we find

$$H_n\geq(1-c)\left[\frac{H_m}{(1-c)}\right]^{(n+1)/(m+1)}\equiv H_{glb}. \tag{B8}$$

Thus, given that the macroscopic potential is known for one value of the hardening exponent (e.g. from a detailed numerical calculation), a lower bound on the potential for another value of the hardening exponent can be easily obtained.

In the special case in which the comparison solid is elastic (i.e. $m = 1$) we find

$$H_1 = \frac{G_m}{\bar{G}}\left(\frac{\Sigma_e}{\sigma_0}\right)^2 \tag{B9}$$

so that

$$H_{glb} = (1-c)\left[\frac{G_m}{\bar{G}(1-c)}\right]^{(n+1)/2}\left(\frac{\Sigma_e}{\sigma_0}\right)^{n+1}. \tag{B10}$$

This corresponds to Ponte Castaneda's original scheme [cf. (41) and (42)] as should be expected. Note that the procedure gives a bound (or an estimate if an approximate result is used for $\bar{G}$ rather than an exact result) for the macroscopic potential which is a function of only the second invariant of the stress deviator. This structure is forced upon the approximate constitutive relation by the choice of comparison solid, but does not necessarily correspond to the structure of the exact constitutive relation.

For axisymmetric stress states, the macroscopic potential depends only on the effective stress and can be written as

$$H = F\left(\frac{\Sigma_e}{\sigma_0}\right)^{n+1} \tag{B11}$$

where the function F depends only on the aspect ratio of the inclusions and the hardening exponent. Assuming that F_m is known (corresponding to a comparison solid with hardening exponent m), then (B8) can be used to obtain

$$F_n \geqslant (1-c)\left[\frac{F_m}{(1-c)}\right]^{(n+1)/(m+1)} \tag{B12}$$

corresponding to a composite with hardening exponent n. In this instance, the bound on the constitutive potential does in fact retain the proper functional dependence on the stress.

Other special cases of loading can be treated similarly to the case of axisymmetric deformation just discussed. For general loading, however, it may not be possible to explicitly state the dependence of H on the invariants of the stress deviator. The relation (B8) represents a bound on the constitutive behavior of the composite, but it does not necessarily predict (or preserve) the correct structure of the constitutive relation in terms of the stress. As already discussed, the procedure developed by Ponte Castaneda (1991) uses a linear comparison solid and this forces the functional form of the macroscopic potential to be in terms of only the effective stress.